

# Boron Carbide (B4C) Reinforced Aluminum Matrix Composites (AMCs)



Daulat Kumar Sharma, Mileend Sharma, Gautam Upadhyay

**Abstract:** Aluminum matrix composites (AMCs) demonstrating a good combination of properties that are hard to acquire by a monolithic aluminum material. Since the last few decades, investigators have shown their keen interest to advance these materials for complex applications. Homogeneous reinforcement distribution, defect-free microstructure, and improved resultant properties depends on the fabrication method along with matrix and reinforcement materials and size. Two-step melt stirring technique and K<sub>2</sub>TiF<sub>6</sub> flux enhanced the wettability and improve the particle distribution of boron carbide (B<sub>4</sub>C) in AMCs. The mechanical properties of the AMCs were enriched by either extrusion process or thermal treatment. Hybrid composites exhibited better characteristics than mono composites. Surface composites manufactured by incorporation of reinforcement in the surface layer; offer good surface properties without losing toughness and ductility. The B<sub>4</sub>C-Al interfacial reactions produce different precipitates in AMCs and damaged the composite's age-hardening ability. B<sub>4</sub>C reinforced friction stir processed surface composites exhibits refined structure and better properties compared to the aluminum matrix. The strength, hardness, and wear resistance of AMCs increased with rising fraction and reducing the size of B<sub>4</sub>C up to a certain level. Wear rate increases with rising applied load, sliding time and speed. A review of effect of B<sub>4</sub>C reinforcement on different properties of mono and hybrid AMCs with summarized results attained and concluded by different investigators is presented in this paper to help researchers in the field. At the end of this paper a position given to conclusions and future directions.

**Keywords:** Aluminum matrix, B<sub>4</sub>C, composites, reinforcement.

## I. INTRODUCTION

Composites deliver a good combination of properties compared to their monolithic counterparts, which governed by fabrication method, grain size, and microstructure along with matrix and reinforcement materials. Metal matrix composites (MMCs) are delivered high-end properties like high strength to weight ratio, high specific strength,

low coefficient of thermal expansion, improved high temperature and electrical performance, better wear, abrasion and corrosion resistance, etc. A good combination of properties unable MMCs to use in automobile, aerospace, electronics, infrastructure, sports, and recreational industries, etc. Aluminum is one of the most used lightweight metal as matrix material in a combination of SiC, TiC, B<sub>4</sub>C, Al<sub>2</sub>O<sub>3</sub>, ZrO<sub>2</sub>, Y<sub>2</sub>O<sub>3</sub>, TiB<sub>2</sub>, Si<sub>3</sub>N<sub>4</sub>, AlN, etc. reinforcements. Greater strength to weight ratio, good corrosion, and tribological properties made ceramic-reinforced aluminum metal matrix composites (AMCs) best popular for applications in different sectors not limited to aviation, automobile, marine, infrastructure, sports, recreation, and defense [1, 2]. B<sub>4</sub>C is a robust material with excellent chemical and thermal stability, high hardness, young's modulus, impact & wear resistance, and low density. Table I exhibited the mechanical and physical properties of B<sub>4</sub>C ceramic particles. Lightweight Al/B<sub>4</sub>C composites exhibited high hardness, low density, and excellent thermal and chemical stability, used in a bicycle frame, bulletproof vests, armor tanks, transportation, containment of nuclear waste, neutron absorber in nuclear power plant, etc. Lightweight AA6061/B<sub>4</sub>C composites are remarkably used in neutron shielding applications owned to its neutron absorbing characteristics and good strength [3, 4]. Since the last few decades, investigators have shown their keen interest in the advanced properties of these materials for complex applications. Hybrid composites incorporate more than one reinforcement material and exhibited better characteristics than mono composites [5-7]. Homogeneous reinforcement distribution, wettability of reinforcement with matrix, and defect-free microstructure are the crucial issues of AMC fabrication. The presence of hard ceramic reinforcements in the soft aluminum matrix falls the toughness and ductility, which restrict extensive applications of AMCs. Surface composites manufactured by the reinforcement only in the surface layer, hence offer good surface properties without decreasing the toughness and ductility of the bulk [8, 9]. This paper exhaustively reviews the effect of B<sub>4</sub>C reinforcement to develop AMCs with advanced properties by different methods. This review paper also signifies the results attained and concluded by different investigators.

**Table I. Mechanical and physical properties of B<sub>4</sub>C ceramic particle.**

Density	Compressive Strength	Knoop hardness	Young's Modulus	Thermal Conductivity	Thermal expansion coefficient
2.52 g/cm <sup>3</sup>	3000 MPa	2800 kg/mm <sup>2</sup>	460 GPa	29 W/m.K	5x10 <sup>-6</sup> /K

**Revised Manuscript Received on November 30, 2019.**

\* Correspondence Author

**Daulat Kumar Sharma\***, Metallurgy Department, Government Engineering College, Gandhinagar 382028, Gujarat, India and Gujarat Technological University, Ahmedabad 382424, Gujarat, India. Email: dksharma.met@gmail.com

**Mileend Sharma**, Mett-Bio Metallurgical Testing & Services, Ahmedabad 382415, Gujarat, India. Email: sharmamps3951@gmail.com

**Gautam Upadhyay**, Gujarat Technological University, Ahmedabad 382424, Gujarat, India. Email: gautam.upadhyay@gmail.com

© The Authors. Published by Blue Eyes Intelligence Engineering and Sciences Publication (BEIESP). This is an [open access](http://creativecommons.org/licenses/by-nc-nd/4.0/) article under the CC-BY-NC-ND license <http://creativecommons.org/licenses/by-nc-nd/4.0/>

### II. AMCs FABRICATION METHODS OVERVIEW

AMCs mainly manufactured by liquid-state processing, solid-state processing, and reactive processing. In liquid-state processing techniques, the reinforcements are incorporated into the molten aluminum matrix. Various methods fall under this group are stir casting, squeeze casting, compocasting, ultrasonic-assisted casting, thermal spray, infiltration, etc. The Stir casting technique is very simple and economical, but it suffers from non-homogeneity in reinforcement distribution and poor wettability of reinforcement and matrix. Good reinforcement distribution along with increased interfacial bonding reported in extruded stir-cast AMCs [10]. Good wettability in between reinforcements and the aluminum matrix reported by the use of preheated reinforcement particles flux [11, 12]. In the stir casting technique, the density difference in the aluminum matrix and reinforcements tend the reinforcement particles to float on the molten aluminum, which fallouts as non-homogeneous distribution. Two-stage addition of reinforcements in aluminum may result in better homogeneous distribution [13, 14]. Ultrasonic treatment is supportive in reducing process time and oxidation, improving particle distribution and matrix-reinforcement bonding [15]. The squeeze cast AMCs exhibited better properties than stir cast [5]. The compo casting process refines the reinforcement particles, improves the reinforcements wettability with the matrix, and advances the reinforcement distribution along with mechanical properties [16]. Rapid solidification in the thermal spray process can prevent particle segregation [17]. The liquid state processing methods also suffer from the formation of detrimental phases due to the reaction of the molten matrix along with reinforcements [18].

To overcome the high-temperature issues of liquid-state processing, AMCs can be manufactured under the aluminum melting temperature; called solid-state processing. This group comprises powder metallurgy, high energy mechanical milling, spark plasma sintering, cold spraying, friction stir processing, etc. Powder metallurgy is the best-preferred manufacturing method for AMCs attributed to more homogeneous microstructure, precise dimensions, and lesser machining operations and scrap cost. The spark plasma sintering technique delivers high heating rates along with reduced sintering time and endorses dense composite with enhanced properties [19, 20]. In the cold spray technique unlike thermal spray powders are not melted under process [21].

In the liquid state processing of surface composites the high temperatures interfacial reaction in matrix and reinforcements resulted in the development of detrimental phases [22]. Solid-state processing of surface composites like friction stir processing (FSP) functions under substrate melting point and uniformly distributed reinforcement particles without any unwanted reactions [23]. In the reactive processing, thermodynamically stable reinforcements are developed in the matrix itself by chemical reactions among various elements, hence also known as in-situ processing. The in-situ processing is economical since it not need costly reinforcement materials as in the case of ex-situ processing methods and supplies better wettability, and reinforcement

distribution [24, 25]. The preferred characteristics and microstructure of fabricated composites, type of reinforcement, size, volume fraction, and matrix material govern the selection of the processing method.

### III. EFFECT OF B4C REINFORCEMENT IN MONO AMCS

Advanced properties of AMCs, particle distribution, and defect-free microstructure along with manufacturing method and matrix material depend on reinforcement materials, type, volume fraction and numbers. The resultant properties advanced by rising B4C fraction and reducing size up to a certain extent. Ubaid et al. [26] produced Al/B4C nanocomposites by microwave sintering method tailed by hot extrusion. Uniform nanoparticles distribution reported. With rising, B4C content coefficient of thermal expansion (CTE) and density decreased whereas porosity, elastic modulus, hardness, and compression and tensile strengths increased. Fig. 1 showed the effect of B4C content on density, porosity, hardness, and CTE. Al/1.0 vol. % B4C exhibited maximum hardness 135.56 Hv, Young's modulus 88.63 GPa, compression strength 524.67 MPa and tensile strength 194.41 Mpa.

The effects of reinforcement content and aging on the microstructure and mechanical behavior of powder metallurgical neutron absorber AA6061/B4C composites observed by Gao et al. [27]. The Mg2Si precipitates marked nearby interfaces with dislocations. With increasing B4C particle content the age-hardening response, ultimate tensile strength and the yield strength improved while the failure strain and electrical conductivity decreased.

Chen et al. [3] prepared AA6061/B4C neutron-absorbing composites with 10%, 20%, 30% and 40% volume fractions by vacuum hot pressing tailed by hot rolling. The neutron transmission ratio reduced with the increased volume fraction of B4C and the plate thickness as shown in Fig. 2a. Uniformly distributed particle, well-bonded interface, refined grains, dislocation around particles, mainly Al and B4C with some AlB2 and Al3BC phases reported. With an increased volume fraction of B4C, the tensile and yield strength first improved and then reduced, whereas elongation decreased as shown in Fig. 2b. The interfacial debonding and particle cleavage fracture were the failure modes of composites.

Singh et al. [28] examined wear mechanisms of stir cast AA5083/B4C composites with 5, 10, 15 and 20 wt. % B4C at 1000 m, 2000 m, and 3000 m sliding distance, 30 N, 40 N and 50 N load and 1 m/s, 2 m/s and 3 m/s sliding velocity. The wear resistance improved with increasing fraction of reinforcement into the matrix and decreased with the rising applied load, sliding speed and distance. Fig. 3 showed the effect of load, and speed on volume loss. The wear rate and the coefficient of friction of AA5083/B4C composites were lesser than the base alloy attributed to improved hardness, refined grains, uniform particle distribution, and reduced porosity. The dominant wear for AA5083 was adhesion while the composite was abrasive.

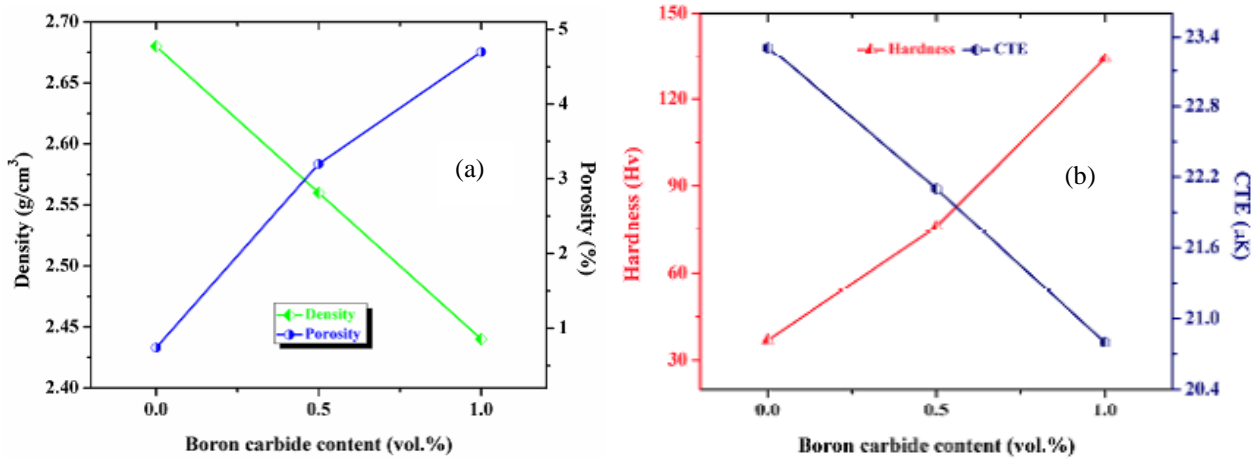


Fig. 1. Effect of B4C content on (a) density and porosity, and (b) hardness and CTE of Al/B4C nanocomposites [26].

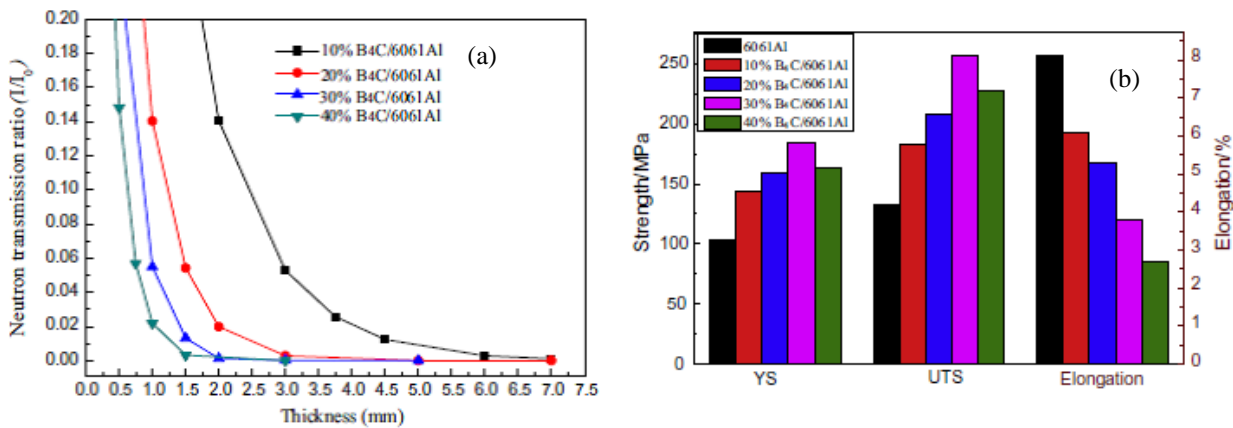


Fig. 2. For the AA6061/B4C neutron-absorbing composite with different B4C contents: (a) relationship between the neutron transmission ratio and thickness, and (b) tensile properties [3].

Effect of reinforcement particle size on the microstructure evolution and mechanical behavior of AA7075/B4C composites studied by Wu et al. [29]. Composites produced by plasma-activated Sintering using three sizes of B4C particles; 56.9  $\mu\text{m}$ , 4.2  $\mu\text{m}$  and 2.0  $\mu\text{m}$ . The coarse particles revealed a comparatively homogeneous particle dispersion, whereas the fine particles revealed particle agglomeration. The finest particle reinforcement displayed the maximum yield and fracture strength attributed to greater strain gradient strengthening and CTE mismatch strengthening.

Poovazhagan et al. [15] used the ultrasonic cavitation supported casting process to produce AA6061/nano-B4C composites. As compared to the unreinforced equivalent, the nanocomposites offered a refined matrix. The nanocomposite presented uniform particle distribution, improved hardness, dry sliding wear resistance, dislocation density, and tensile strength, through holding a decent amount of alloy ductility and impact resistance. Fig. 4 displayed the effect of nano-B4C particle reinforcement on the hardness and wear loss of composite. Shorowordi et al. [10] incorporated 6–20 vol. % reinforcement to produce Al/B4C, Al/SiC and Al/Al<sub>2</sub>O<sub>3</sub> stir-cast composites with different Stirring time, and extruded them to improve particle distribution and interfacial bonding. Paralleled to Al/ Al<sub>2</sub>O<sub>3</sub> and Al/SiC composites, Al/B4C composites exhibited superior particle distribution and better interfacial bonding. For a long processing time, interfacial reaction products predicted only at the Al/SiC interface as

shown in Fig. 5. Al<sub>2</sub>O<sub>3</sub> and Al<sub>3</sub>BC, two secondary phases found away from the Al/B4C interface.

AA6061/30 wt.% B4C neutron-absorbing composites were manufactured by Chen et al. [4] using the powder metallurgy route. A reasonably homogeneous B4C particle distribution with B4C, Al and Al<sub>2</sub>O<sub>3</sub> phases in the composite was reported. B4C particles stimulated dynamic recrystallization (DRX) nucleation and restrict the Al grain growth and preferential orientation. With increasing deformation, the ultimate tensile strength and yield strength first improved and then reduced, however B4C particle fracture along with huge stress concentration about the B4C particles decreased elongation. Chen et al. [30] observed the impact of compositional gradient on microstructure evolution and properties of a spark plasma sintered AA6061/B4C laminar composite. The composite extruded and hot rolled and reasonably distributed particles with well-bonded interfaces in absence of porosity in transition regions between different layers reported. Around B4C particles grains were smaller compared to away from the B4C particles. Ultimate tensile strength and yield strength of the rolled composite were improved but elongation was decreased compared to extrude composite. Strengthening mechanisms in the composites were dislocation strengthening, grain refinement, load transfer effect, and Orowan mechanism.

## Boron Carbide (B<sub>4</sub>C) Reinforced Aluminum Matrix Composites (AMCs)

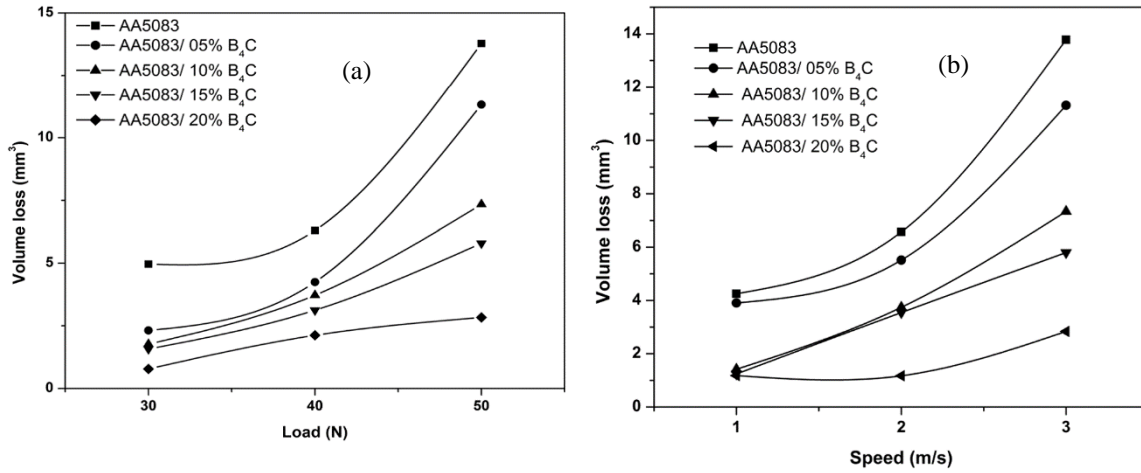


Fig. 3. Effect of (a) load, and (b) speed on volume loss of AA5083/B<sub>4</sub>C Composites [28].

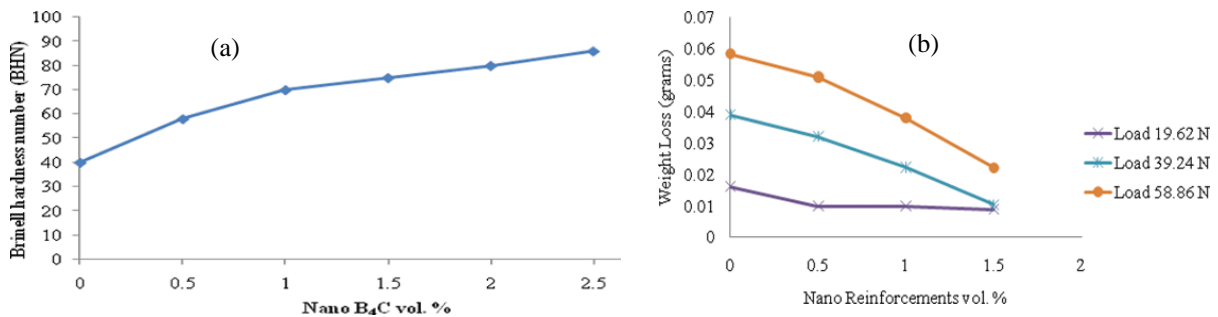


Fig. 4. Effect of nano-B<sub>4</sub>C particle reinforcement on (a) hardness and (b) wear of AA6061/nano-B<sub>4</sub>C composite [15].

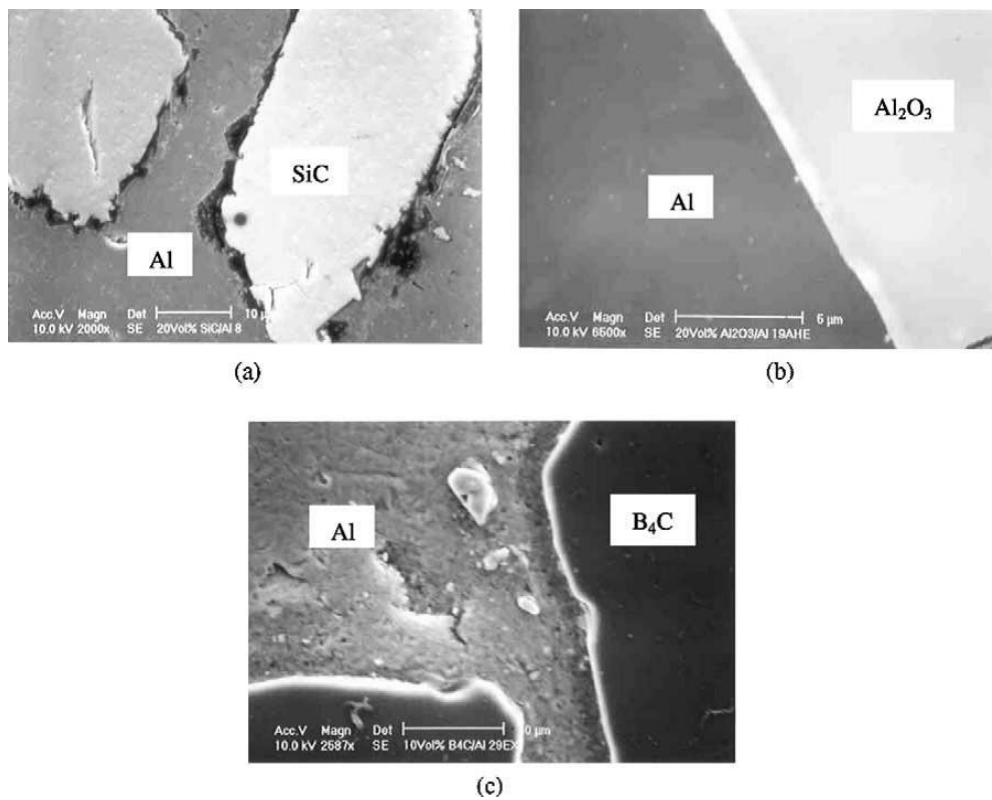


Fig. 5. SEM micrographs showing the interfaces of (a) Al/20 vol.% SiC (interaction time 60 min), (b) Al/20 vol.% Al<sub>2</sub>O<sub>3</sub> (interaction time 66 min) and (c) Al/13 vol.% B<sub>4</sub>C (interaction time 46 min) [10].

Effect of heat treatment, applied load, sliding time and velocity on the friction and wear behavior of stir cast AA6061/20 wt.%B4C composite examined by Dou et al. [31]. In the primary stage of wear test, the mass loss showed proportional behavior with the applied load and sliding time, whereas it reduces slightly by an increase of the sliding velocity. At 240 rpm sliding velocity, 120 min sliding time, and 30 N applied a load, the severe delamination wear takes place with extensively increased mass loss and coefficient of friction. The composite displayed maximum wear resistance after 1 h solutionizing at 550 °C and 15 h aging at 180 °C as shown in Fig. 6 by Mg<sub>2</sub>Si precipitation and improved Al-B4C interface bonding.

Toptan et al. [11] fabricated stir cast composites using 10 wt% B4C reinforcement, and AA6063 and AA1070 matrix. K<sub>2</sub>TiF<sub>6</sub> flux used to improve the wettability of B4C with liquid alloy. Reasonably homogeneous particle distribution exhibited by both AMCs. The addition of the flux enhanced the wettability by the development of very thin TiC and TiB<sub>2</sub> reaction layers.

Auradi et al. [13] used two-step adding melt stirring technique and K<sub>2</sub>TiF<sub>6</sub> flux to advance wettability and to escape particle agglomeration in the production of AA6061/B4C composites with 5 and 7wt% reinforcements. Better particle distribution in absence of agglomeration, enhanced hardness, tensile strength, and compression strength were revealed by the composites. Table II displays the degree of development in tensile and compression strength of the AA6061 by reinforcement of B4C particles. α-Al, B4C and minor Al<sub>3</sub>Ti and Al<sub>3</sub>BC phases shown in XRD of the composites. Al<sub>3</sub>Ti phase confirms the Ti compound/layer made around the reinforcement particles B4C.

Zhou et al. [32] produced AA6061/26 wt.% B4C composites by powder metallurgy with 560°C and 620°C hot-pressed temperature and examine the role of the microalloying element Cu in composites. The B4C-Al interfacial reactions produce Al<sub>3</sub>BC and MgB<sub>2</sub> precipitates in composites and replaced the Q phase which was the leading Cu-contained precipitate in the absence of the interfacial reaction. Cu segregation at the precipitates/matrix interface drops the interfacial free energy and rise the precipitate nucleation.

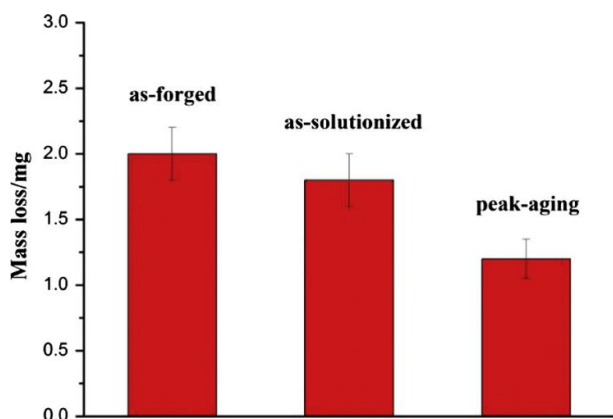


Fig. 6. Mass loss of AA6061/20 wt.%B4C composites after different heat treatments (20 N, 120 rpm, 60 min) [31].

**Table II.** The degree of development in tensile and compression strength of the AA6061 by reinforcement of B4C particles manufactured by two-stage adding melt stirring at 750 °C temperature [13].

Composition	The improvement in ultimate tensile strength (%)	The improvement in compression strength (%)
6061Al + 5wt% B4CP	22.124	12.761
6061Al + 7wt% B4CP	38.812	32.068

Li et al. [33] studied the interfacial reaction mechanism in AA6061/B4C composites produced by the powder metallurgy route. Complicated interfacial reactions arose in the AA601/B4C composites and formed Al<sub>3</sub>BC, MgB<sub>7</sub>, MgAl<sub>2</sub>O<sub>4</sub>, Mg<sub>0.78</sub>Al<sub>10.75</sub>B<sub>14</sub>, Al<sub>4</sub>SiC<sub>4</sub>, and AlB<sub>12</sub>C<sub>2</sub>, which weakened the composites age-hardening ability.

Zan et al. [34] produced AA6061/B4C composites by varied hot-pressing temperatures powder metallurgy methods. The interfacial reactions develop Al<sub>3</sub>BC and Mg(Al)B<sub>2</sub> compounds and improve the mechanical properties through increased hot-pressing temperatures from 560 °C to 630 °C. The 630 °C hot-pressed sample exhibited 40~59% higher tensile strength than 560 °C hot-pressed at both room temperature and elevated temperatures as Mg(Al)B<sub>2</sub> nanorods hinder the dislocations movements. The mechanical properties of the 630 °C hot-pressed samples were steady for 400 °C annealing up to 8000 h. The high temperatures stable, high strength, economical Al-B4C neutron absorber materials required for the dry storage of spent nuclear fuels.

Yuvaraj et al. [35] produced Al5083/B4C surface composite by FSP. Surface composites exhibit fine grain size, higher hardness, Ultimate tensile strength (UTS) & wear resistance compare to Al alloy. Increased FSP passes uniformly distribute nanoparticles in the matrix. Reinforcement of B4C nanoparticles showed better microhardness and wear resistance than B4C micro-particles.

Rana et al. [8] fabricated Al/B4C surface composite by FSP and examined the effect of particle reinforcement strategies on the microstructure and resultant properties. More homogeneous B4C dispersion detected in AA6061 compared to AA7075, whereas the best dispersion was perceived by using fine powder and by a change in FSP pass direction. Almost doubled hardness and wear resistance of AA7075/B4C composites reported. AA7075/B4C surface composite produced by Tonelli et al. [36] using FSP. Rising FSP passes results in improved B4C distribution and the presence of B4C particles enhanced the wear resistance of the Al alloy and raise the friction coefficient. Table III summarizes the effect of B4C reinforcement in different mono AMCs fabricated by various methods.

## Boron Carbide (B4C) Reinforced Aluminum Matrix Composites (AMCs)

**Table III. Summary of the effect of B4C reinforcement in different mono AMCs.**

Author	Method	Substrate	Reinforcement	Prominent results/effect
Dou et al. [31]	Stir casting	AA6061	B4C	In the primary stage of wear test, the mass loss showed proportional behavior with the applied load and sliding time, whereas it reduces slightly by an increase of the sliding velocity. The composite displayed maximum wear resistance after 1 h solutionizing at 550 °C and 15 h aging at 180 °C.
Shorowordi et al. [10]	Stir casting	Pure Al	SiC (40 μm), α-Al <sub>2</sub> O <sub>3</sub> (32 μm), B <sub>4</sub> C (40 μm)	Compared to Al/SiC and Al/Al <sub>2</sub> O <sub>3</sub> composites, Al/B <sub>4</sub> C composites exhibited superior particle distribution and better interfacial bonding. For a long processing time, interfacial reaction products predicted only at the Al/SiC interface. Al <sub>2</sub> O <sub>3</sub> and Al <sub>3</sub> BC, two secondary phases found away from the Al/B <sub>4</sub> C interface.
Toptan et al. [11]	Stir casting	AA 1070, AA 6063	B <sub>4</sub> C particles (32 μm)	Reasonably homogeneous particle distribution exhibited by both AMCs. The addition of the flux enhanced the wettability by the development of very thin TiC and TiB <sub>2</sub> reaction layers.
Auradi et al. [13]	Two-step addition melt stirring	AA6061	B <sub>4</sub> C particles (88 μm)	Better particle distribution in absence of agglomeration, enhanced hardness, tensile strength, and compression strength was revealed by the composites. Al <sub>3</sub> Ti phase confirms the Ti compound/layer made around the reinforcement particles B <sub>4</sub> C.
Poovazhagan et al. [15]	Ultrasonic cavitation assisted casting	AA6061	B <sub>4</sub> Cp (50 nm)	The nanocomposite presented uniform particle distribution, improved hardness, dry sliding wear resistance, dislocation density, and tensile strength, through holding a decent amount of alloy ductility and impact resistance.
Zhou et al. [32]	Powder metallurgy	AA6061	B <sub>4</sub> C	The B <sub>4</sub> C-Al interfacial reactions produce Al <sub>3</sub> BC and MgB <sub>2</sub> precipitates in composites. Cu segregation at the precipitates/matrix interface drops the interfacial free energy and rise the precipitate nucleation.
Zan et al. [34]	High energy ball milling	AA6061 powder (13 μm)	B <sub>4</sub> C (7 μm)	The interfacial reactions develop Al <sub>3</sub> BC and Mg(Al)B <sub>2</sub> compounds and improve the mechanical properties through increased hot-pressing temperatures from 560 °C to 630 °C. The 630 °C hot-pressed sample exhibited 40~59% higher tensile strength than 560 °C hot-pressed at both room temperature and elevated temperatures.
Gao et al. [27]	High energy ball milling	AA6061 powder (13 μm)	B <sub>4</sub> C (7 μm)	The Mg <sub>2</sub> Si precipitates marked nearby interfaces with dislocations. With increasing B <sub>4</sub> C particle content the age-hardening response, ultimate tensile strength and the yield strength improved while the failure strain and electrical conductivity decreased.
Li et al. [33]	Powder metallurgy	AA6061 (13 μm)	B <sub>4</sub> C (7 μm)	Complicated interfacial reactions arose in the AA601/B <sub>4</sub> C composites and formed Al <sub>3</sub> BC, MgB <sub>7</sub> , MgAl <sub>2</sub> O <sub>4</sub> , Mg <sub>0.78</sub> Al <sub>10.75</sub> B <sub>14</sub> , Al <sub>4</sub> Si <sub>4</sub> C <sub>4</sub> , and AlB <sub>12</sub> C <sub>2</sub> , which weakened the composites age-hardening ability.
Chen et al. [3]	vacuum hot pressing tailed by hot rolling	AA6061 (14 μm)	B <sub>4</sub> C (23 μm)	The neutron transmission ratio reduced with the increased volume fraction of B <sub>4</sub> C and the plate thickness. Uniformly distributed particle, well-bonded interface, refined grains, dislocation around particles, mainly Al and B <sub>4</sub> C with some AlB <sub>2</sub> and Al <sub>3</sub> BC phases reported. With increased volume fraction of B <sub>4</sub> C, the tensile and yield strength first improved and then reduced, whereas elongation decreased
Chen et al. [4]	Powder metallurgy	AA6061 (13 μm)	B <sub>4</sub> C (0-44 μm)	A reasonably homogeneous B <sub>4</sub> C particle distribution with B <sub>4</sub> C, Al and Al <sub>2</sub> O <sub>3</sub> phases in the composite was reported. With increasing deformation, the ultimate tensile strength and yield strength first improved and then reduced, however, elongation decreased.
Chen et al. [30]	Spark plasma sintering, extrusion, hot rolling	AA6061 (13 μm)	B <sub>4</sub> C (0-44 μm)	Reasonably distributed particles with well-bonded interfaces in absence of porosity in transition regions between different layers reported. Ultimate tensile strength and yield strength of the rolled composite was improved but elongation were decreased compared to extruded composite.
Singh et al. [28]	stir-casting	AA5083	B <sub>4</sub> C (300 mesh)	The wear resistance improved with increasing reinforcement into the matrix and decreased with the rising applied load, sliding speed and distance. The wear rate and the coefficient of friction of AA5083/B <sub>4</sub> C composites were lesser than the base alloy. The dominant wear for AA5083 was adhesion while the composite was abrasive.
Ubaid et al. [26]	Microwave sintering, hot extrusion	Pure Al (~7-15 μm)	B <sub>4</sub> C (~10 nm)	With rising, B <sub>4</sub> C content coefficient of thermal expansion and density decreased whereas porosity, elastic modulus, hardness, and compression and tensile strengths increased. Uniform nanoparticles distribution reported.
Wu et al. [29]	Plasma activated sintering	AA7075 (29.3 μm)	B <sub>4</sub> C (56.9 μm, 4.2 μm and 2.0 μm)	The coarse particles revealed a comparatively homogeneous particle dispersion, whereas the fine particles revealed particle agglomeration. The finest particle reinforcement displayed the maximum yield and fracture strength.
Yuvaraj et al. [35]	Friction stir processing	Al alloy 5083-O	B <sub>4</sub> C (20 μm and 30-60 nm)	Surface composites exhibit fine grain size, higher hardness, UTS & wear resistance compare to Al alloy. The reinforcement of B <sub>4</sub> C nanoparticles showed better microhardness and wear resistance than B <sub>4</sub> C micro-particles.
Rana et al. [8]	Friction stir processing	AA7075-T 651 and AA6061	B <sub>4</sub> C (8-12 μm) & (15-18 μm)	AA6061 exhibited more homogeneous B <sub>4</sub> C dispersion compared to AA7075, whereas the best dispersion was observed by using fine powder and change in FSP direction. Nearly double hardness and wear resistance of AA7075/B <sub>4</sub> C composites reported.
Tonelli et al. [36]	Friction stir processing	AA7075-O	B <sub>4</sub> C (20 μm)	Rising FSP passes results in improved B <sub>4</sub> C distribution and the presence of B <sub>4</sub> C particles enhanced the wear resistance of the Al alloy and raise the friction coefficient.

### IV. EFFECT OF B4C REINFORCEMENT IN HYBRID AMCS

More than one reinforcement material incorporate in hybrid composites to combined properties of different reinforcements. Hybrid composites exhibited better characteristics than their mono composite counterparts. Kumaran et al. [37] studied dry sliding wear of stir cast AA6351/5 wt% SiC+5 wt% and 10 wt% B<sub>4</sub>C composites.

The friction and wear of the composites affected by the applied load, sliding velocity and B<sub>4</sub>C wt%. Kumaran et al. [38] examined the effect of B<sub>4</sub>C particles on the wear behavior of stir cast AA6351/5 wt.% SiC composite. With higher wt. % of B<sub>4</sub>C particles,

composites can preserve the wear resistance at higher load and velocity. The B4C particles made a strong interface bond and preserved the surface against severe destruction.

Baradeswaran et al. [39] reinforced 10 wt.% B4C and 5 wt.% graphite in AA6061 and AA7075 by liquid casting route. The AA7075 hybrid composite displayed better hardness and elongation compared to AA6061 hybrid composite. The composites exhibited improved wear resistance attributed to MML on the worn surfaces. The mathematical models formulated using response surface regression (RSM) analysis which showed a minimum wear rate at 10N applied load, 0.8 m/s sliding speed, and 2000 m distance. AA 7075 hybrid composite shown better tribological behavior.

Stir cast hybrid composites AA6061/SiC+B4C manufactured by Das et al. [40]. As shown in Fig. 7, wear rate of composites established a proportional relationship with the

applied load and found maximum at 30 N load and of 500 rpm sliding speed. Temperature increase with sliding speed softens the matrix and initiates the wear. The compact contact area between the mating surfaces caused by the presence of ceramic particles in the matrix resulted in the decreased coefficient of friction with both increased normal load and sliding speed. The dominant wear was oxidation, abrasion, and adhesion.

Uthayakumar et al. [14] examined pin on disc dry sliding wear behavior of AA100/5% SiC+ 5% B4C hybrid composite at varying load 20–100 N and sliding velocities 1-5 m/s. The two-step stir cast hybrid composites exhibited uniform particle distribution and improved wear resistance. The composites showed improved wear resistance up to 60 N load and 1–4 m/s sliding speeds as shown in Fig. 8.

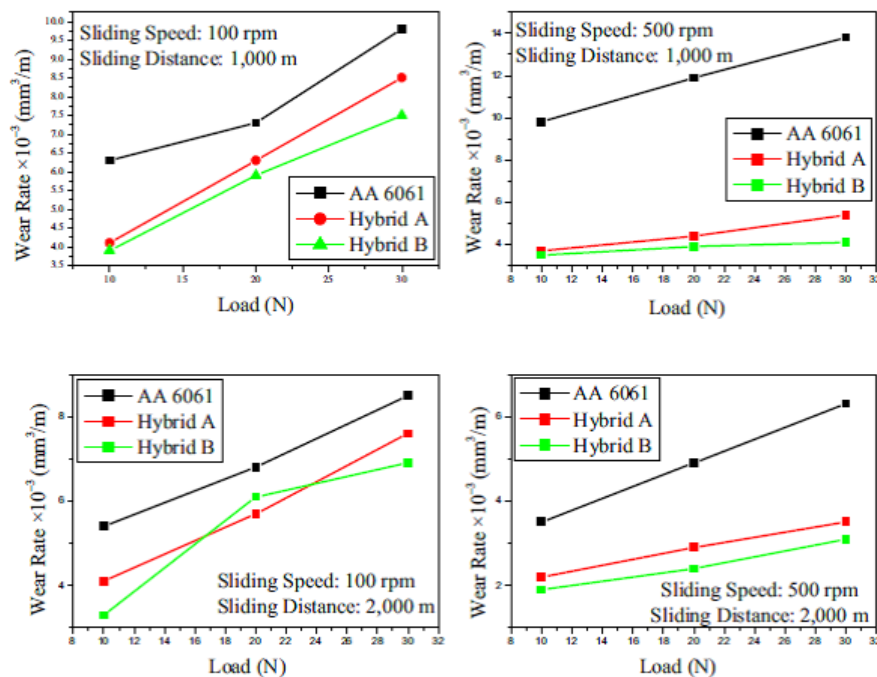


Fig. 7. Wear rate vs applied load at different sliding speed and distance for as received AA6061, hybrid composite A: AA6061/0.5 wt% SiC+1.5 wt% B4C, and hybrid composite B: 1.5 wt% SiC+1.5 wt% B4C [40].

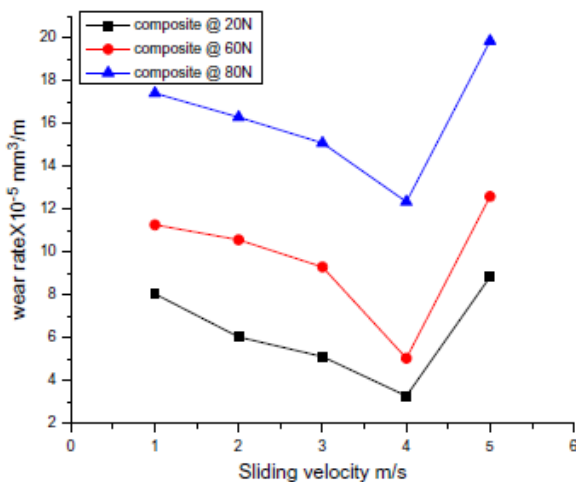


Fig. 8. Effect of sliding velocity and load on wear rate of AA100/5% SiC+5% B4C hybrid composites [14].

Hariprasad et al. [41] examined the wear behavior of Al5083/Al2O3+B4C hybrid composites and reported

upgraded wear resistance. The light adhesive wear traces exhibited by the worn samples. Kumar et al. [42] fabricated stir cast nanocomposites Al2219/B4C, and Al2219/B4C+MoS2. Uniform distribution of particles and increased microhardness with a fraction of n-B4C/MoS2 particles reported. The n-B4C particles and increased feed rate improve the surface roughness and cutting force, whereas decreases by increased cutting speed. The machined surface showed plastic deformation and abrasion marks.

Sharma et al. [23] produced mono AA6061/B4C and hybrid AA6061/B4C+MoS2 surface composites by the FSP route and reported Uniform particle distribution and highest hardness acquired by AA6061/B4C whereas highest wear resistance by AA6061/75%B4C +25%MoS2. Yuvaraj et al. [43] produced AA5083/ B4C+TiC hybrid surface composites by FSP and reported even dispersion of particles and refined grains.

## Boron Carbide (B4C) Reinforced Aluminum Matrix Composites (AMCs)

The Al/B4C surface composite showed maximum microhardness whereas Al/B4C+TiC hybrid composite showed maximum wear resistance. Wear rate increases with increasing load.

Pol et al. [44] processed AA7005/B4C+TiB<sub>2</sub> hybrid composites by FSP and reported uniform particle distribution. Hybrid composites displayed improved hardness, ballistic resistance, and ballistic mass efficiency factor attributed to dispersion strengthening by particle reinforcement. Patle et al. [45] fabricated mono AA7075/B4C and AA7075/B4C+

MoS<sub>2</sub> hybrid surface composite by FSP. All processed samples showed lower hardness than base alloy AA7075 due to the intermetallic strengthening phase dissolution by FSP. Heat-treated samples showed improved hardness and heat-treated AA7075/B4C+MoS<sub>2</sub> hybrid composite revealed the highest wear resistance due to solid lubricant MoS<sub>2</sub>. Table IV summarizes the effect of B4C reinforcement in different hybrid AMCs fabricated by various methods.

**Table IV. Summary of the effect of B4C reinforcement in different hybrid AMCs.**

Author	Method	Substrate	Reinforcements	Prominent results/effect
Das et al. [40]	Stir casting	AA6061	SiC and B4C (both 50 nm)	The wear rate of composites established a proportional relationship with the applied load. The presence of ceramic particles resulted in the decreased coefficient of friction with both increased normal load and sliding speed. The dominant wear was oxidation, abrasion, and adhesion.
Uthayakumar et al. [14]	two step stir casting	AA1100	SiC (10 μm), B4C (65 μm)	The two-step stir cast hybrid composites exhibited uniform particle distribution and improved wear resistance up to 60 N load and 1–4 m/s sliding speeds.
Hariprasad et al. [41]	stir casting	Al 5083	n-Al <sub>2</sub> O <sub>3</sub> , B4C (400 μm)	Improved wear resistance of hybrid composites.
Kumar et al. [42]	stir casting process	Al-Cu binary alloy Al2219	n-B4C (30–60 nm), MoS <sub>2</sub> (600–900 nm)	The n-B4C particles and rising feed rate improve the surface roughness and cutting force, whereas drop by increased cutting speed. The machined surface showed plastic deformation & abrasion marks.
Baradeswaran et al. [39]	liquid casting route	AA6061 & AA7075	B4C and graphite (both 16–20 μm)	The AA7075 hybrid composite displayed better hardness and elongation compared to AA6061 hybrid composite. The composites exhibited improved wear resistance. AA 7075 hybrid composite shown better tribological behavior.
Kumaran et al. [37]	stir casting	AA6351	SiC and B4C	The friction and wear of the composites affected by the applied load, sliding velocity and B4C wt%.
Kumaran et al. [38]	stir casting	AA6351	SiC and B4C	At higher B4C fraction, composites can preserve the wear resistance at higher load and velocity. The B4C particles made a strong interface bond and preserved the surface against severe destruction.
Sharma et al. [23]	Friction stir processing	AA6061-T 651	B4C (8 μm) and MoS <sub>2</sub> (3 μm)	Uniform particle distribution and highest hardness acquired by AA6061/B4C whereas highest wear resistance by AA6061/75%B4C+25%MoS <sub>2</sub> .
Yuvaraj et al. [43]	Friction stir processing	AA5083-O	B4C and TiC (both 30–60 nm)	Even dispersion of particles and refined grains. The Al/B4C showed maximum microhardness whereas Al/B4C+TiC maximum wear resistance. Wear rate increases with increasing load.
Pol et al. [44]	Friction stir processing	AA7005 (	B4C and TiB <sub>2</sub> ( both 3 μm)	Uniform particle distribution. Hybrid composites displayed improved hardness, ballistic resistance, and ballistic mass efficiency factor.
Patle et al. [45]	Friction stir processing	AA7075-T 6	B4C (10–15 μm) and MoS <sub>2</sub> (60–80 nm)	All processed samples showed lower hardness than base alloy AA7075 however heat-treated samples showed improved hardness and heat-treated AA7075/B4C+MoS <sub>2</sub> hybrid composite revealed highest wear resistance.

## V. CONCLUSION AND FUTURE DIRECTIONS

AMCs can be processed to present outstanding properties by the use of different reinforcement materials and processing routes, and satisfy various industrial requirements that cannot be attained by conventional materials. The fabrication method, material, size, number, and the fraction of reinforcement, and matrix material governs the advanced properties of AMCs.

AMCs exhibited improved hardness, wear resistance, tensile and compression strength and decreased friction coefficient, which further upgraded by rising reinforcement content. The key conclusions made from the works carried out by different researchers are as:

- In AMCs with rising B4C content coefficient of thermal expansion, density, failure strain, and electrical conductivity decrease whereas porosity, elastic modulus, hardness, wear resistance, age-hardening response, and compression, tensile and yield strengths increases. Wear rate increases with rising applied load, sliding time and speed. In the AA6061/B4C neutron-absorbing composites, the neutron transmission ratio reduced with the increased volume fraction of B4C.

- Compared to Al/SiC and Al/Al<sub>2</sub>O<sub>3</sub> composites, Al/B4C composites exhibited superior particle distribution and better interfacial bonding.
- Compare to the coarse particles, fine particles exhibited better yield and fracture. Reinforcement of nano-B4C particles showed better microhardness and wear resistance than micro-B4C particles. The nano-AMCs offered refined matrix, uniform particle distribution, improved hardness, wear resistance, dislocation density, and tensile strength while retaining a decent amount of ductility and impact resistance of matrix.
- Two-step melt stirring technique and K<sub>2</sub>TiF<sub>6</sub> flux enhanced the wettability and improve the particle distribution in B4C reinforced AMCs. In the extruded and hot-rolled AMCs the particle distribution, interface bonding, tensile and yield strength was improved whereas porosity and elongation were decreased.
- The B4C-Al interfacial reactions produce different precipitates in AMCs, which weakened the composite's age-hardening ability. B4C reinforced friction stir processed (FSPed) surface composites exhibit fine grain size, higher hardness,

UTS & wear resistance compare to Al matrix. Increased FSP passes, change in direction and more fine powder results in more uniform particle distribution in the matrix.

- More than one reinforcements in hybrid AMCs delivers better properties than single reinforcement in mono AMCs. The FSPed hybrid composite displayed better hardness, tribological behavior, ballistic resistance, and ballistic mass efficiency factor compared to mono composite.
- The FSPed AA7075 hybrid composite displayed better hardness, elongation, and tribological behavior compared to AA6061 hybrid composite, however more homogeneous B4C dispersion detected in AA6061 compared to AA7075. In the T6 treated Al alloys the strengthening phase dissolve by FSP and resulted in the lower hardness of FSPed samples which can be improved by heat treatment.

The creation of undesired phases, particle distribution and accumulation, and wettability of reinforcement with the matrix are the key issues in AMCs development. Homogeneous particle distribution is challenging to manage by a liquid metallurgy route. Investigators in the field should focus on cost-effective AMC production procedures, surface alteration techniques, and materials.

## REFERENCES

1. Idusuyi N, Olayinka JI. Dry sliding wear characteristics of aluminium metal matrix composites: a brief overview. *Journal of Materials Research and Technology*. 2019.
2. Miracle D. Metal matrix composites—from science to technological significance. *Composites science and technology*. 2005;65(15-16):2526-40.
3. Chen H, Wang W, Li YL, Zhang P, Nie H, Wu Q. The design, microstructure and tensile properties of B4C particulate reinforced 6061Al neutron absorber composites. *Journal of Alloys and Compounds*. 2015;632:23-9.
4. Chen H, Wang W, Nie H, Zhou J, Li Y, Liu R, et al. Microstructure evolution and mechanical properties of B4C/6061Al neutron absorber composite sheets fabricated by powder metallurgy. *Journal of Alloys and Compounds*. 2018;730:342-51.
5. Kannan C, Ramanujam R. Comparative study on the mechanical and microstructural characterisation of AA 7075 nano and hybrid nanocomposites produced by stir and squeeze casting. *Journal of advanced research*. 2017;8(4):309-19.
6. Sharma VK, Kumar V, Joshi RS. Experimental investigation on effect of RE oxides addition on tribological and mechanical properties of Al-6063 based hybrid composites. *Materials Research Express*. 2019.
7. Padmavathi K, Ramakrishnan R. Tribological behaviour of aluminium hybrid metal matrix composite. *Procedia Engineering*. 2014;97:660-7.
8. Rana H, Badheka V, Kumar A, Satyaprasad A. Strategic parametric investigation on manufacturing of Al–Mg–Zn–Cu alloy surface composites using FSP. *Materials and Manufacturing Processes*. 2018;33(5):534-45.
9. Mishra RS, Ma Z. Friction stir welding and processing. *Materials science and engineering: R: reports*. 2005;50(1-2):1-78.
10. Shorowordi KM, Laoui T, Haseeb A, Celis J-P, Froyen L. Microstructure and interface characteristics of B4C, SiC and Al<sub>2</sub>O<sub>3</sub> reinforced Al matrix composites: a comparative study. *Journal of Materials Processing Technology*. 2003;142(3):738-43.
11. Toptan F, Kilicarslan A, Karaaslan A, Cigdem M, Kerti I. Processing and microstructural characterisation of AA 1070 and AA 6063 matrix B4Cp reinforced composites. *Materials & Design*. 2010;31:S87-S91.
12. Ramesh M, Ravichandran M. Investigation on Mechanical Properties and Wear Behaviour of Titanium Diboride Reinforced Composites. *FME Transactions*. 2019;47:873-9.
13. Auradi V, Rajesh G, Kori S. Preparation, Characterization and Evaluation of Mechanical Properties of 6061Al-Reinforced B4C Particulate Composites via Two-Stage Melt Stirring. *Materials and Manufacturing Processes*. 2014;29:194-200.
14. Uthayakumar M, Aravindan S, Rajkumar K. Wear performance of Al–SiC–B4C hybrid composites under dry sliding conditions. *Materials & Design*. 2013;47:456-64.
15. Poovazhagan L, Kalaichelvan K, Sornakumar T. Processing and performance characteristics of aluminum-nano boron carbide metal matrix nanocomposites. *Materials and Manufacturing Processes*. 2016;31(10):1275-85.
16. Amirkhanlou S, Niroumand B. Synthesis and characterization of 356-SiCp composites by stir casting and compocasting methods. *Transactions of nonferrous metals society of china*. 2010;20:s788-s93.
17. Aussavy D, Costil S, El Kedim O, Montavon G, Bonnot A-F. Metal matrix composite coatings manufactured by thermal spraying: Influence of the powder preparation on the coating properties. *Journal of Thermal Spray Technology*. 2014;23(1-2):190-6.
18. Lai S-W, Chung D. Consumption of SiC whiskers by the Al–SiC reaction in aluminium-matrix SiC whisker composites. *Journal of Materials Chemistry*. 1996;6(3):469-77.
19. Al-Aqeeli N, Mohammad K, Laoui T, Saheb N. The effect of variable binder content and sintering temperature on the mechanical properties of WC–Co–VCr<sub>3</sub>C<sub>2</sub> nanocomposites. *Materials and Manufacturing Processes*. 2015;30(3):327-34.
20. Azam MU, Ahmed BA, Hakeem AS, Irshad HM, Laoui T, Ehsan MA, et al. Tribological behaviour of alumina-based nanocomposites reinforced with uncoated and Ni-coated cubic boron nitride. *Journal of Materials Research and Technology*. 2019:14.
21. Gyansah L, Tariq N, Tang J, Qiu X, Feng B, Huang J, et al. Cold spraying SiC/Al metal matrix composites: effects of SiC contents and heat treatment on microstructure, thermophysical and flexural properties. *Materials Research Express*. 2018;5(2):026523.
22. Pantelis D, Tissandier A, Manolatos P, Ponthiaux P. Formation of wear resistant Al–SiC surface composite by laser melt–particle injection process. *Materials science and technology*. 1995;11(3):299-303.
23. Sharma DK, Patel V, Badheka V, Mehta K, Upadhyay G. Fabrication of hybrid surface composites AA6061/(B4C+ MoS<sub>2</sub>) via friction stir processing. *Journal of Tribology*. 2019;141(5):052201.
24. Selvam JDR, Dinaharan I, Philip SV, Mashinini P. Microstructure and mechanical characterization of in situ synthesized AA6061/(TiB<sub>2</sub>+ Al<sub>2</sub>O<sub>3</sub>) hybrid aluminum matrix composites. *Journal of Alloys and Compounds*. 2018;740:529-35.
25. David Raja Selvam J, Dinaharan I, Rai RS, Mashinini P. Role of zirconium diboride particles on microstructure and wear behaviour of AA7075 in situ aluminium matrix composites at elevated temperature. *Tribology-Materials, Surfaces & Interfaces*. 2019:1-9.
26. Ubaid F, Matli P, Shakoor R, Parande G, Manakari V, Mohamed A, et al. Using B4C nanoparticles to enhance thermal and mechanical response of aluminum. *Materials*. 2017;10(6):621.
27. Gao M, Kang H, Chen Z, Guo E, Peng P, Wang T. Effect of reinforcement content and aging treatment on microstructure and mechanical behavior of B4Cp/6061Al composites. *Materials Science and Engineering: A*. 2019;744:682-90.
28. Singh R, Shadab M, Dash A, Rai R. Characterization of dry sliding wear mechanisms of AA5083/B 4 C metal matrix composite. *Journal of the Brazilian Society of Mechanical Sciences and Engineering*. 2019;41(2):98.
29. Wu C, Ma K, Wu J, Fang P, Luo G, Chen F, et al. Influence of particle size and spatial distribution of B4C reinforcement on the microstructure and mechanical behavior of precipitation strengthened Al alloy matrix composites. *Materials Science and Engineering: A*. 2016;675:421-30.
30. Chen H-s, Wang W-x, Nie H-h, Zhou J, Li Y-l, Zhang P. Microstructure and mechanical properties of B4C/6061Al laminar composites fabricated by power metallurgy. *Vacuum*. 2017;143:363-70.
31. Dou Y, Liu Y, Liu Y, Xiong Z, Xia Q. Friction and wear behaviors of B4C/6061Al composite. *Materials & Design*. 2014;60:669-77.
32. Zhou Y, Zan Y, Zheng S, Wang Q, Xiao B, Ma X, et al. Distribution of the microalloying element Cu in B4C-reinforced 6061Al composites. *Journal of Alloys and Compounds*. 2017;728:112-7.
33. Li Y, Wang Q, Wang W, Xiao B, Ma Z. Interfacial reaction mechanism between matrix and reinforcement in B4C/6061Al composites. *Materials Chemistry and Physics*. 2015;154:107-17.
34. Zan Y, Zhang Q, Zhou Y, Wang Q, Xiao B, Ma Z. Enhancing high-temperature strength of B4C–6061Al neutron absorber material by in-situ Mg (Al) B<sub>2</sub>. *Journal of Nuclear Materials*. 2019:151788.
35. Yuvaraj N, Aravindan S. Fabrication of Al5083/B4C surface composite by friction stir processing and its tribological characterization. *Journal of materials research and technology*. 2015;4(4):398-410.

## Boron Carbide (B4C) Reinforced Aluminum Matrix Composites (AMCs)

36. Tonelli L, Morri A, Toschi S, Shaaban M, Ammar H, Ahmed M, et al. Effect of FSP parameters and tool geometry on microstructure, hardness, and wear properties of AA7075 with and without reinforcing B 4 C ceramic particles. The International Journal of Advanced Manufacturing Technology. 2019;102(9-12):3945-61.
  37. Thirumalai Kumaran S, Uthayakumar M, Aravindan S. Analysis of dry sliding friction and wear behaviour of AA6351–SiC–B4C composites using grey relational analysis. Tribology-Materials, Surfaces & Interfaces. 2014;8(4):187-93.
  38. Thirumalai Kumaran S, Uthayakumar M, Aravindan S, Rajesh S. Dry sliding wear behavior of SiC and B4C-reinforced AA6351 metal matrix composite produced by stir casting process. Proceedings of the Institution of Mechanical Engineers, Part L: Journal of Materials: Design and Applications. 2016;230(2):484-91.
  39. Baradeswaran A, Vettivel S, Perumal AE, Selvakumar N, Issac RF. Experimental investigation on mechanical behaviour, modelling and optimization of wear parameters of B4C and graphite reinforced aluminium hybrid composites. Materials & Design. 2014;63:620-32.
  40. Das S, Chandrasekaran M, Samanta S, Kayaroganam P, Davim P. Fabrication and tribological study of AA6061 hybrid metal matrix composites reinforced with SiC/B4C nanoparticles. Industrial Lubrication and Tribology. 2019.
  41. Hariprasad T, Varatharajan K, Ravi S. Wear characteristics of B4C and Al2O3 reinforced with Al 5083 metal matrix based hybrid composite. Procedia Engineering. 2014;97:925-9.
  42. Kumar NS, Shankar GS, Basavarajappa S, Suresh R. Some studies on mechanical and machining characteristics of Al2219/n-B4C/MoS2 nano-hybrid metal matrix composites. Measurement. 2017;107:1-11.
  43. Yuvaraj N, Aravindan S. Wear characteristics of Al5083 surface hybrid nano-composites by friction stir processing. Transactions of the Indian Institute of Metals. 2017;70(4):1111-29.
  44. Pol N, Verma G, Pandey R, Shanmugasundaram T. Fabrication of AA7005/TiB2-B4C surface composite by friction stir processing: Evaluation of ballistic behaviour. Defence Technology. 2019;15(3):363-8.
  45. Patle H, Mahendiran P, Sunil BR, Dumpala R. Hardness and sliding wear characteristics of AA7075-T6 surface composites reinforced with B4C and MoS2 particles. Materials Research Express. 2019;6(8):086589.
- Ph. D. research work (2006) on “Studies on Silver-Metal Oxide Powder Metallurgical Electrical Contact Materials Prepared by Mechanical Alloying” at the Faculty of Technology and Engineering, M. S. University, Baroda, Gujarat. He has obtained his postgraduate degree in Material Science (1994) from the Indian Institute of Technology, Bombay, Maharashtra, India and an undergraduate degree in Metallurgy (1980) from the Faculty of Technology and Engineering, M. S. University, Baroda, Gujarat. He has published more than 10 research papers in national/international journals and conferences and written 03 books in the material science area. He has thirty-eight years of teaching and industrial experience and given services to many universities for syllabus, recruitment, examinations, etc. He is a member of ASM International and Society of Automotive Engineers, India.

### AUTHORS PROFILE



**Daulat Kumar Sharma** is working as Assistant Professor, Metallurgy Engineering, Government Engineering College, Gandhinagar, Gujarat, India and pursuing Ph. D. from Gujarat Technological University Ahmedabad, Gujarat. He has published 06 research papers in national/international journals and conferences

and written 01 book chapter based on experimental results of sliding wear behavior of mechanically alloyed Al-Si-SiCp nanocomposites. He has more than thirteen years of teaching and research experience. He has obtained his postgraduate degree in Non-Ferrous Metallurgy (2006) from Malaviya National Institute of Technology (MNIT), Jaipur, Rajasthan, India. He is a life member of the Indian Institute of Metals, Indian Institute of Welding, Materials Research Society of India, and Indian Society for Technical Education. Currently, he is working on surface composite manufacturing through friction stir processing.



**Mileend Sharma** has obtained his undergraduate degree in metallurgy engineering (2019) from Government Engineering College, Gandhinagar, Gujarat affiliated to Gujarat Technological University, Ahmedabad, Gujarat, India. During his undergraduate studies, he has worked on surface composite manufacturing and surface

modification of aluminum alloys through friction stir processing route. He had done several internships and vocational trainings in reputed industries and testing labs. He had also completed NDT level two course in visual testing, liquid penetrant testing, magnetic particle testing, ultrasonic testing, and radiographic testing. Currently, he is working in a NABL accredited testing house, Mett-Bio metallurgical testing & services, Ahmedabad, Gujarat.



**Dr. Gautam Upadhyay** is working as Principal, D. A. Degree Engineering and Technology, Mahemdabad, Gujarat, India affiliated to Gujarat Technological University, Ahmedabad, Gujarat. He has completed his